PROCEEDINGS OF THE ROYAL SOCIETY A

rspa.royalsocietypublishing.org

Research

Article submitted to journal

Subject Areas:
Composite materials, Homogenization

Keywords:
Effective properties, Potential problem, Antiplane elasticity, Homogenization

Author for correspondence:
William J. Parnell
e-mail:
william.parnell@manchester.ac.uk

Royal Society Publishing
Informing the science of the future

An integral equation method for the homogenization of unidirectional fibre reinforced media; antiplane elasticity and other potential problems.

Duncan Joyce, William J. Parnell, Raphael Assier and I. David Abrahams

School of Mathematics, University of Manchester, Oxford Road, Manchester, M13 9PL

In Parnell and Abrahams (2008 *Proc. Roy. Soc. A* 464, 1461-1482) (doi:10.1098/rspa.2007.0254) a homogenization scheme was developed that gave rise to explicit, analytical forms for the effective antiplane shear modulus of a periodic fibre reinforced medium. The expressions take the form of rational functions in the volume fraction ϕ. In that scheme a (non-dilute) approximation was invoked in order to determine simple leading order expressions and it was shown that agreement with existing methods is good except at very high volume fractions. Here the theory is extended in order to determine higher order terms in the rational function expansions.

The methodology is attractive in that the expressions can be derived for a large class of fibres with non-circular cross section. Furthermore, terms are clearly identified as being associated with the lattice geometry of the periodic structure, fibre cross-sectional shape, and host/fibre material properties. The expressions are derived in the context of antiplane elasticity but the analogy with the potential problem illustrates the broad applicability of the method to, e.g., thermal, electrostatic and magnetostatic problems. The efficacy of the scheme is illustrated by comparison with the well-established method of asymptotic homogenization where the associated cell problem is usually solved by some computational scheme, e.g. finite element methods.

1. Introduction

A classical problem in the mechanics of inhomogeneous media is to attempt to replace the two-dimensional potential problem $\nabla \cdot (\mu(\boldsymbol{x})\nabla w(\boldsymbol{x})) = 0$, where

$\boldsymbol{x} = (x_1, x_2)$ and $\mu(\boldsymbol{x})$ is a periodic (scalar) function that varies rapidly with $\boldsymbol{x}$, by an equivalent problem of the form

$$\nabla \cdot (\boldsymbol{\mu}_* \nabla w_*(\boldsymbol{x})) = 0. \tag{1.1}$$

In order to do this, a so-called *separation of scales* between the micro and macro lengthscales must be assumed and in general the *effective property* $\boldsymbol{\mu}_*$ is a second order tensor with components μ_{*ij} in the context of Cartesian coordinates, for example. The path to (1.1) is the process of *homogenization* and $\boldsymbol{\mu}_*$ depends strongly on the geometrical and physical properties of the medium in question [1,2]. Noting that the equations arise from the equilibrium equation $\nabla \cdot \boldsymbol{\sigma} = 0$ where $\boldsymbol{\sigma} = \boldsymbol{\mu e}$, and $\boldsymbol{e} = \nabla w$, it is stressed that the problem posed has broad applicability, as summarized in Table 1. To fix ideas here the application to antiplane elasticity shall be described.

Assume now that $\mu(\boldsymbol{x})$ is piecewise constant, and a cross-section of the medium takes the form as depicted in Fig. 1 so that the material can be classified as a unidirectional fibre-reinforced composite (FRC), noting that general fibre cross-sections shall be considered. Such media are used in a multitude of applications where rather specific material properties are required in order to perform a task effectively and where frequently naturally available homogeneous media are not effective or efficient [1]. In particular materials of this form can provide high tensile stiffness and/or high directional conductivity whilst remaining relatively light by using only a small volume fraction of the fibre phase.

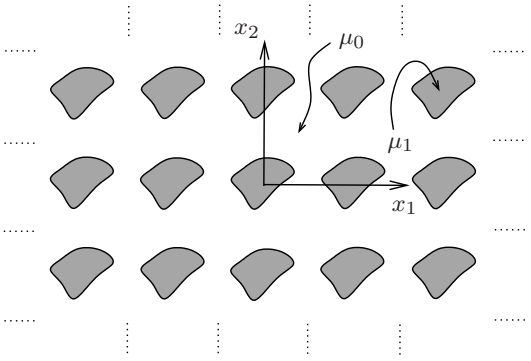

Figure 1: An inhomogeneous medium with piecewise constant material property $\mu(\boldsymbol{x})$. The unidirectional fibre reinforced composite medium depicted here has general microstructure, in particular the fibres have non-circular cross-sections.

The microstructural lengthscales of such inhomogeneous media are becoming ever smaller with an increasing ability to engineer microstructures for improved macroscopic performance [3]. It is frequently convenient to consider the problem in the context of wave propagation so that an inertia term is added to the governing equation and the effective medium is then governed by, for example

$$\nabla \cdot (\boldsymbol{\mu}_* \nabla w_*(\boldsymbol{x})) + \rho_* \omega^2 w_*(\boldsymbol{x}) = 0, \tag{1.2}$$

where in the context of antiplane elasticity ρ_* is the effective mass density and where time-harmonic motion $e^{-i\omega t}$ has been assumed, where ω is the angular frequency. By considering this dynamic context, a natural macroscopic lengthscale is introduced: the wavelength of the propagating effective wave. Intrinsic to the subject of homogenization then, where quasi-static properties are determined, is that the wavelength of the propagating wave is much longer than the microstructural lengthscale.

A number of methods have proved extremely successful at predicting $\boldsymbol{\mu}_*$ in both the static and quasi-static regimes, including the method of asymptotic homogenization [2,4–6], the equivalent inclusion method [7,8], boundary element solutions of integral equations [9] and the use of Fourier transforms [10–12]. All schemes rely on the separation of scales and periodicity - the fact that a periodic cell is representative of the entire medium. A significant amount of work has been done that incorporates propagation at finite frequencies and particularly when the wavelength of the propagating wave is of the order of the microstructure, when dynamic effects become important. In this context the microstructure can be designed to manipulate the wave

Application	σ_i	e_i	w	μ_{ij}
Antiplane elasticity	Antiplane stress vector $(\sigma_{13}, \sigma_{23})$	Displacement gradient ∇w	displacement w	Shear moduli μ_{ij}
Thermal conductivity	Heat flux q_i	Temperature gradient $-\nabla T$	temperature T	thermal conductivity k_{ij}
Electrical conductivity	Electrical current J_i	Electric field $E_i = \nabla \Phi$	Electric potential Φ	Electrical conductivity $\overline{\sigma}_{ij}$
Dielectrics	Displacement field D_i	Electric field $E_i = \nabla \Phi$	Electric potential Φ	Electric permittivity ϵ_{ij}
Magnetism	Magnetic induction B_i	Magnetic field $H_i = \nabla \Psi$	Magnetic potential Ψ	Magnetic permeability μ_{ij}
Porous media	Weighted velocity ηv_i	Pressure gradient ∇p	Pressure p	Permeability k_{ij}
Diffusion	Diffusion flux j_i	Concentration gradient ∇c	Concentration c	Diffusivity D_{ij}

Table 1: Table illustrating the numerous application areas associated with the potential problem, together with corresponding variables. Here attention is restricted to two-dimensional problems.

carrying capabilities of the medium. In particular for periodic materials the microstructure can be chosen in order that the medium acts as a wave filter, for waves in certain frequency ranges (so-called stop bands) waves are forbidden to propagate. Methods devised to determine the so-called band gap structure are the plane wave expansion technique [13], multipole methods [14], and so-called *high frequency homogenization* [15]. See the useful review by [16] for further details. Low frequency effective properties can thus be deduced numerically from these schemes by considering propagation near the origin of the dispersion curves in question. If from the outset however, one is interested purely in the low-frequency limit where homogenization applies, then there is no need to determine this full dynamic behaviour.

Here then a strict separation of scales shall be assumed; the homogenization regime is assumed to hold and the material responds as an effective medium with uniform properties. The key novelty of the proposed scheme is the form of solutions that are derived as shall be illustrated below. The method to be discussed extends the work in [17] (referred to as PA below), where a new homogenization scheme was devised based on the integral equation form of the governing equation, considering antiplane wave propagation in the low frequency limit, so that an equation of the form (1.2) was derived, and the leading order result was determined. The work of PA was itself inspired by the method introduced in [18], in which expressions for the effective elastic properties of three-dimensional random particulate media were determined, but restricted to the dilute-dispersion limit. Returning to the two-dimensional periodic medium considered here, attention shall be restricted to the case of macroscopically orthotropic media, so that $\mu_{*ij} = \delta_{1i}\delta_{1j}\mu_1^* + \delta_{2i}\delta_{2j}\mu_2^*$ when written with respect to the principal axes of anisotropy. In PA the effective moduli were shown to take the following rational function form at leading order:

$$\mu_j^* = \frac{1 + \mathcal{C}_{1j}\phi}{1 + \mathcal{D}_{1j}\phi}. \tag{1.3}$$

The coefficients $\mathcal{C}_{1j}$ and $\mathcal{D}_{1j}$ depend upon the shape of the fibre cross section and the ratio of fibre to host shear moduli. Upon extending the method to higher orders, it shall be shown in this work that for *circular cylindrical fibres* the following result is derived:

$$\mu_j^* = \frac{1 + \mathcal{C}_{1j}\phi + C_{4j}\phi^4 + C_{6j}\phi^6 + C_{7j}\phi^7 + C_{8j}\phi^8 + \ldots}{1 + \mathcal{D}_{1j}\phi + C_{4j}\phi^4 + C_{6j}\phi^6 + C_{7j}\phi^7 + C_{8j}\phi^8 + \ldots} \tag{1.4}$$

and additional general expressions are determined for fibres of more complex cross-section. In principle the scheme presented can be extended to three dimensions and more complex microstructural geometries.

As in PA it shall be assumed that all fibres in the composite are identical, that all phases are isotropic and that the lattice geometry and fibre cross-sections are restricted such that the effective medium appears to be, at most, orthotropic on the macroscale. In Section 2 the governing equations are summarized and the associated integral equations are derived. The integral equation methodology is then described in Section 3 and the manner in which effective properties are determined is presented in Section 4. Results are given in Section 5 for a variety of media before a concluding in Section 6. Some of the more detailed analysis is presented in Appendices in order to aid the flow of the paper.

It is reiterated that although the method is described here in the context of antiplane elasticity and expressions for the effective antiplane shear moduli μ_1^* and μ_2^* are derived, the method is equally applicable to any of the applications summarized in Table 1.

2. Governing Equations

The microstructure of the medium in question is illustrated in Figure 1. Unidirectional fibres, considered so long as for the problem to be assumed two-dimensional, are positioned on a periodic lattice and their cross-section is considered general with the restriction that the macroscopic anisotropy is at most orthotropic. The problem shall be formulated in Cartesian coordinates, with the x_3 coordinate running parallel to the fibre axis and the x_1x_2 plane being the plane of periodicity. The location of the centre of the (s, t)th periodic cell is defined by the lattice vector

$$\boldsymbol{R}(s,t) = q(s\boldsymbol{l}_1 + t\boldsymbol{l}_2), \quad s,t \in \mathbb{Z}, \tag{2.1}$$

for some vectors $\boldsymbol{l}_1, \boldsymbol{l}_2 \in \mathbb{R} \times \mathbb{R}$. Attention is restricted to the case where each periodic cell contains a single fibre. The lengthscale q can be considered as the characteristic lengthscale of the periodic cell and therefore the microstructure of the medium. Consider a distribution of fibres that induces macroscopic *orthotropy* so that

$$\boldsymbol{l}_1 = (A_1, B_1), \quad \boldsymbol{l}_2 = (0, B_2), \quad A_1, B_1, B_2 \in \mathbb{R},$$

and the periodic cell is a parallelogram with area $q^2\mathcal{R} = q^2A_1B_2$. Each cell therefore consists of a fibre of general cross-section occupying the domain V_{st} embedded within the host phase which is denoted by V_0. The shear modulus and mass density of the host (fibre) is denoted as μ_0 (μ_I) and ρ_0 (ρ_I) respectively.

The lengthscale a associated with the fibre cross-section is introduced by defining the boundary of the fibre cross-section in terms of circular cylindrical coordinates, i.e.

$$r(\theta) = af(\theta), \quad \theta \in [0, 2\pi], \tag{2.2}$$

with $f(\theta) \geq 1$ so that $a = \min_{\theta\in[0,2\pi]}(r(\theta))$ on the boundary of the fibre. This choice is convenient for calculations that will be carried out in Appendix A associated with incorporating the *shape* of the fibre cross-section into the analysis.

Horizontally polarized shear (SH) waves, otherwise known as antiplane waves, are considered to propagate through the medium. The associated time-harmonic elastic displacement, polarized in the x_3 direction is denoted by $w(\boldsymbol{x})$, where it is recalled that $\boldsymbol{x} = (x_1, x_2)$. The elastic displacement w is governed by

$$\nabla^2 w(\boldsymbol{x}) + (k_0^2 + (k_1^2 - k_0^2)\chi(\boldsymbol{x}))w(\boldsymbol{x}) = 0, \tag{2.3}$$

where $\nabla = (\partial/\partial x_1, \partial/\partial x_2)$ and where $k_0 = \omega/c_0$ and $k_I = \omega/c_I$ are the wavenumbers of the host and fibre respectively and where $c_0^2 = \mu_0/\rho_0$ and $c_I^2 = \mu_I/\rho_I$ are the squares of the phase velocities

of the two phases. The so-called *indicator function* $\chi(\boldsymbol{x})$ is defined by

$$\chi(\boldsymbol{x}) = \begin{cases} 1 & \text{if } \boldsymbol{x} \in V_{st}, \quad s,t \in \mathbb{Z} \\ 0 & \text{if } \boldsymbol{x} \in V_0. \end{cases}$$

The associated Green's function for the host domain satisfies

$$(\nabla^2 + k_0^2)G(\boldsymbol{x}-\boldsymbol{y}) = \delta(\boldsymbol{x}-\boldsymbol{y}), \tag{2.4}$$

and is

$$G(\boldsymbol{x}-\boldsymbol{y}) = \frac{1}{4i}H_0^{(1)}(k_0|\boldsymbol{x}-\boldsymbol{y}|),$$

where $H_0^{(1)}(r)$ denotes the Hankel function of the first kind and zeroth order.

Combining (2.3) and (2.4) appropriately, imposing boundary conditions of continuity of displacement and traction on fibre/host interfaces, the problem is restated in integral equation form as

$$w(\boldsymbol{x}) = \sum_{\substack{s,t=-\infty \\ s,t\in\mathbb{Z}}}^{\infty} \left(\frac{(\rho_0-\rho_I)\omega^2}{\mu_0} \int_{V_{st}} w(\boldsymbol{y})G(\boldsymbol{y}-\boldsymbol{x})d\boldsymbol{y} - \frac{(\mu_0-\mu_I)}{\mu_0} \int_{V_{st}} \nabla_y w(\boldsymbol{y}) \cdot \nabla_y G(\boldsymbol{y}-\boldsymbol{x})d\boldsymbol{y} \right),$$

where $\nabla_y = (\partial/\partial y_1, \partial/\partial y_2)$. Non-dimensionalising using the scalings $\hat{\boldsymbol{x}} = q\boldsymbol{x}$ and $\hat{w} = w/\hat{W}$, with $\hat{W}$ being a typical displacement magnitude, and noting that Green's function is already non-dimensional, the lattice vector in scaled coordinates becomes

$$\boldsymbol{p} = s\boldsymbol{l}_1 + t\boldsymbol{l}_2,$$

and the cross-sectional area of the periodic cell is $\mathcal{R} = A_1 B_2$. At this point it appears convenient to define the volume fraction per unit span in the x_3 direction, $\phi = |D|/\mathcal{R}$, where $|D|$ is the (non-dimensional) cross-sectional area of the fibre.

Upon dropping the hat notation the non-dimensional integral equation takes the form

$$w(\boldsymbol{x}) = \sum_{\substack{s,t=-\infty \\ s,t\in\mathbb{Z}}}^{\infty} \left((1-d)\varepsilon^2 \int_{V_{st}} w(\boldsymbol{y})G_\varepsilon(\boldsymbol{y}-\boldsymbol{x})d\boldsymbol{y} - (1-m) \int_{V_{st}} \nabla_y w(\boldsymbol{y}) \cdot \nabla_y G_\varepsilon(\boldsymbol{y}-\boldsymbol{x})d\boldsymbol{y} \right), \tag{2.5}$$

where $d = \rho_I/\rho_0$ and $m = \mu_I/\mu_0$ are the contrasts in mass density and shear moduli, $\varepsilon = qk_0$ and

$$G_\varepsilon(\boldsymbol{x}-\boldsymbol{y}) = \frac{1}{4i}H_0(\varepsilon|\boldsymbol{x}-\boldsymbol{y}|).$$

Note that

$$\lim_{\varepsilon\to 0} G_\varepsilon(\boldsymbol{x}-\boldsymbol{y}) = \frac{1}{2\pi}\ln(|\boldsymbol{x}-\boldsymbol{y}|) + \gamma_c = G_0(\boldsymbol{x}-\boldsymbol{y}) + \gamma_c \tag{2.6}$$

where $\gamma_c = \frac{2\gamma_e - i\pi - 2\log 2}{4\pi}$ is a constant and $\gamma_e = 0.577216...$ is Euler's constant. Having already dropped hats, referring to (2.2), in non-dimensional coordinates the boundary of the fibre is therefore described by $r = \ell f(\theta), \quad \theta \in [0, 2\pi]$, where $\ell = a/q$. The non-dimensional fibre cross-section is easily shown to be

$$|D| = \int_0^{2\pi}\int_0^{\ell f(\theta)} r\,dr\,d\theta = \frac{\ell^2}{2}\int_0^{2\pi} f^2(\theta)d\theta$$

and the *volume fraction* of the fibre cross section within the periodic cell is then

$$\phi = \frac{|D|}{\mathcal{R}} = \frac{\ell^2}{2\mathcal{R}}\int_0^{2\pi} f^2(\theta)d\theta.$$

Therefore

$$\ell = \sqrt{2\mathcal{R}\phi \Big/ \int_0^{2\pi} f^2(\theta)d\theta} = \tau\sqrt{\phi}. \tag{2.7}$$

Attention here is restricted to the scenario where τ remains $O(1)$, with respect to ϕ. Therefore from (2.7),

$$\ell = O(\sqrt{\phi}). \tag{2.8}$$

In the homogenization regime $ak_0 \ll 1$ and $\varepsilon = qk_0 \ll 1$ and it can be assumed here that $ak_0 = O(\varepsilon)$. In [19,20] the regime where $ak_0 \ll 1$ but ε is not restricted to being small was considered. Note that this requires $\phi \ll 1$. If one wished, the method introduced in the next section could be modified in order to consider this regime.

3. The Integral Equation Method

In PA it was shown that setting $m = 1$ leads to the result $\rho_* = (1-\phi) + d\phi$ for the non-dimensional effective density (scaled on ρ_0) in the quasi-static limit. This is an exact result in the separation of scales regime. Here, without loss of generality and in order to determine the effective shear modulus, set $d = 1$ in (2.5). Differentiate both sides of the resulting integral equation with respect to $x_k, k = 1, 2$ to yield

$$\frac{\partial w}{\partial x_k}(\boldsymbol{x}) = -(1-m) \sum_{\substack{s,t=-\infty \\ s,t\in\mathbb{Z}}}^{\infty} \left(\frac{\partial}{\partial x_k} \int_{V_{st}} \nabla_y w(\boldsymbol{y}) \cdot \nabla_y G_\varepsilon(\boldsymbol{y}-\boldsymbol{x}) d\boldsymbol{y} \right). \tag{3.1}$$

Now take $\boldsymbol{x} \in V_{ab}$, i.e. within the (a, b)th fibre, which has position vector $\boldsymbol{r} = a\boldsymbol{l}_1 + b\boldsymbol{l}_2$. By taking the Taylor expansion of Green's function about the point $\boldsymbol{y} = \boldsymbol{p} = (p_1, p_2) = s\boldsymbol{l}_1 + t\boldsymbol{l}_2$ (i.e. about the centre of the(s, t)th fibre), (3.1) becomes

$$\begin{aligned} \partial_{x_k} w(\boldsymbol{x}) = (1-m) \sum_{\substack{s,t=-\infty \\ (s,t)\neq(a,b)}}^{\infty} \left(\sum_{n=1}^{2} \sum_{i,j=0}^{\infty} W_{ij}^{(n)}(\boldsymbol{p}) \left(\partial_{y_n} \partial_{y_k} \partial_{y_1}^i \partial_{y_2}^j G_\varepsilon(\boldsymbol{y}-\boldsymbol{x}) \right) \Big|_{\boldsymbol{y}=\boldsymbol{p}} \right) \\ - (1-m) \partial_{x_k} \int_{V_{ab}} \nabla_y w(\boldsymbol{y}) \cdot \nabla_y G_\varepsilon(\boldsymbol{y}-\boldsymbol{x}) d\boldsymbol{y}, \end{aligned} \tag{3.2}$$

where $\partial_{y_k}^i$ denotes the i^{th} derivative with respect to y_k and

$$W_{ij}^{(k)}(\boldsymbol{p}) = \int_{V_{st}} \frac{1}{i!j!} (y_1 - p_1)^i (y_2 - p_2)^j \frac{\partial w}{\partial y_k}(\boldsymbol{y}) d\boldsymbol{y} = O(\phi^{(i+j+2)/2}). \tag{3.3}$$

The variables introduced as $W_{ij}^{(k)}(\boldsymbol{p})$ can be thought of as *displacement-gradient moments* of order $i + j$, recalling that $\phi = |D|/\mathcal{R}$. The order of these moments has been deduced using the fact that, since w is a smooth function, w and all its derivatives will be $O(1)$.

Notice that the term for $(s, t) = (a, b)$ is not included in the summation, nor has the Taylor series of the Green's function been taken in this term, because Green's function is singular in the domain V_{ab} since $\boldsymbol{x}$ is contained in this region. The assumption that one can Taylor expand Green's function puts restrictions upon the parameters ε and ϕ. Either (a) $\varepsilon \ll 1$ in which case ϕ is unrestricted *or* (b) $\varepsilon = O(1)$ and then $\phi \ll 1$ is required. Here only the scenario of (a) is considered.

Proceed now by defining the operation $\mathcal{L}_{\delta\xi}[(*)]$ as the act of multiplying each side of equation $(*)$ by $(x_1 - r_1)^\delta (x_2 - r_2)^\xi / (\delta!\xi!)$ and integrating in the $\boldsymbol{x}$ plane over the domain V_{ab}, where $\boldsymbol{r} = (r_1, r_2)$. Hence consider $\mathcal{L}_{\delta\xi}[(3.2)]$ and Taylor expand Green's function and its derivatives about $\boldsymbol{x} = \boldsymbol{r}$ to obtain, after some rearrangement

$$\begin{aligned} \frac{W_{\delta\xi}^{(k)}(\boldsymbol{r})}{(m-1)} + \sum_{\boldsymbol{p}\neq\boldsymbol{r}} \left(\sum_{n=1}^{2} \sum_{i,j,\alpha,\beta=0}^{\infty} W_{ij}^{(n)}(\boldsymbol{p}) C_{\delta\xi\alpha\beta} \left(\partial_{y_n} \partial_{y_k} \partial_{y_1}^{i+\alpha} \partial_{y_2}^{j+\beta} G_\varepsilon(\boldsymbol{y}-\boldsymbol{x}) \right) \Big|_{\boldsymbol{x}=\boldsymbol{r},\boldsymbol{y}=\boldsymbol{p}} \right) \\ = \mathcal{A}_{\delta\xi}^{(k)}(\boldsymbol{r}), \end{aligned} \tag{3.4}$$

where the property $\partial G_\varepsilon/\partial x_k = -\partial G_\varepsilon/\partial y_k$ has been employed. Furthermore, the following terms have been defined:

$$\mathcal{A}^{(k)}_{\delta\xi}(\boldsymbol{r}) = \int_{V_{ab}} \frac{(x_1 - r_1)^\delta (x_2 - r_2)^\xi}{\delta!\xi!} \partial_{x_k} \int_{V_{ab}} \nabla_y w(\boldsymbol{y}) \cdot \nabla_y G_\varepsilon(\boldsymbol{y} - \boldsymbol{x}) d\boldsymbol{y} d\boldsymbol{x} \tag{3.5}$$
$$= O(\phi^{(\delta+\xi+2)/2})$$

and

$$C_{\delta\xi\alpha\beta} = \int_{V_{ab}} \frac{(-1)^{\alpha+\beta}}{\alpha!\beta!\delta!\xi!} (x_1 - r_1)^{\delta+\alpha} (x_2 - r_2)^{\xi+\beta} d\boldsymbol{x} \tag{3.6}$$
$$= \int_0^{2\pi} \int_0^{\ell f(\hat{\theta})} \frac{(-1)^{\alpha+\beta} R^{\delta+\alpha+\xi+\beta+1}}{\alpha!\beta!\delta!\xi!} (\cos\Theta)^{\delta+\alpha} (\sin\Theta)^{\xi+\beta} dR d\Theta$$
$$= \frac{(-1)^{\alpha+\beta} \ell^{\delta+\alpha+\xi+\beta+2}}{\alpha!\beta!\delta!\xi!(\delta+\alpha+\xi+\beta+2)} \int_0^{2\pi} [f(\Theta)]^{\delta+\alpha+\xi+\beta+2} (\cos\Theta)^{\delta+\alpha} (\sin\Theta)^{\xi+\beta} d\Theta$$
$$= \ell^{\delta+\alpha+\xi+\beta+2} \hat{C}_{\delta\xi\alpha\beta}, \tag{3.7}$$

where the local polar coordinate system $x_1 = R\cos\Theta, x_2 = R\sin\Theta$ has been defined and where (2.7) is used in order to define $\hat{C}_{\delta\xi\alpha\beta} = O(1)$. As was shown in PA the influence of the cross-sectional shape of the fibre is embedded *solely* in the terms known as the *shape tensors* $\mathcal{A}^{(k)}_{\delta\xi}$, the form of which shall be considered shortly.

(a) The shape factor

The term $\mathcal{A}^{(k)}_{\delta\xi}$ incorporating fibre cross-section in (3.5) appears to possess a singularity at $\boldsymbol{y} = \boldsymbol{x}$ due to the presence of derivatives of Green's function in the integrand. However, as was shown in [17], this apparent singular contribution is found to be zero by splitting the domain V_{ab} up into a non-singular part $V_{ab}\backslash C_\psi$ and apparently singular part C_ψ, where C_ψ is a circle of radius $\psi \ll 1$ with origin $\boldsymbol{y} = \boldsymbol{x}$. Therefore all that remains to consider are integrals of the type

$$\mathcal{A}^{(k)}_{\delta\xi}(\boldsymbol{r}) = \lim_{\psi\to 0} \int_{V_{ab}} \frac{(x_1 - r_1)^\delta (x_2 - r_2)^\xi}{\delta!\xi!} \partial_{x_k} \int_{V_{ab}\backslash C_\psi} \nabla_y w(\boldsymbol{y}) \cdot \nabla_y G_\varepsilon(\boldsymbol{y} - \boldsymbol{x}) d\boldsymbol{y} d\boldsymbol{x}. \tag{3.8}$$

Once again employing the property $\partial G_\varepsilon/\partial x_k = -\partial G_\varepsilon/\partial y_k$, the x_k derivative may be taken inside the $\boldsymbol{y}$ integral, and since the range of integration does not include the region where $G(\boldsymbol{y} - \boldsymbol{x})$ is singular, exchanging the order of integration is permissable. Therefore

$$\mathcal{A}^{(k)}_{\delta\xi}(\boldsymbol{r}) = -\lim_{\psi\to 0} \int_{V_{ab}\backslash C_\psi} \partial_{y_1} w(\boldsymbol{y}) \partial_{y_k} \partial_{y_1} J_{\delta\xi}(\boldsymbol{y}) + \partial_{y_2} w(\boldsymbol{y}) \partial_{y_k} \partial_{y_2} J_{\delta\xi}(\boldsymbol{y}) d\boldsymbol{y}, \tag{3.9}$$

where

$$J_{\delta\xi}(\boldsymbol{y}) = \int_{V_{ab}} \frac{(x_1 - r_1)^\delta (x_2 - r_2)^\xi}{\delta!\xi!} G_\varepsilon(\boldsymbol{y} - \boldsymbol{x}) d\boldsymbol{x}. \tag{3.10}$$

It is convenient here to represent (3.10) as a series expansion, i.e.

$$J_{\delta\xi} = D^{\delta\xi}_{00} + D^{\delta\xi}_{10}(y_1 - r_1) + D^{\delta\xi}_{01}(y_2 - r_2) + \sum_{p=2}^{\mathcal{P}+2} \sum_{q=0}^{p} \left(\frac{D^{\delta\xi}_{(p-q)q}}{(p-q)!q!} (y_1 - r_1)^{p-q} (y_2 - r_2)^q \right) \tag{3.11}$$

so that displacement gradient moments naturally arise in (3.9). A procedure for obtaining the coefficients $D^{\delta\xi}_{ij}$ for a given fibre cross-section is outlined in Appendix A. The order of truncation, $\mathcal{P} + 2$ is governed by the shape function f involved. For elliptical fibres $\mathcal{P} = \delta + \xi$ for example.

Substituting (3.11) into (3.10) and (3.9) and adjusting the indices one obtains

$$\mathcal{A}^{(1)}_{\delta\xi}(\boldsymbol{r}) = -\sum_{p=0}^{\mathcal{P}}\sum_{q=0}^{p}\left(D^{\delta\xi}_{(p-q+2)q}W^{(1)}_{(p-q)q}(\boldsymbol{r}) + D^{\delta\xi}_{(p-q+1)(q+1)}W^{(2)}_{(p-q)q}(\boldsymbol{r})\right), \tag{3.12}$$

$$\mathcal{A}^{(2)}_{\delta\xi}(\boldsymbol{r}) = -\sum_{p=0}^{\mathcal{P}}\sum_{q=0}^{p}\left(D^{\delta\xi}_{(p-q+1)(q+1)}W^{(1)}_{(p-q)q}(\boldsymbol{r}) + D^{\delta\xi}_{(p-q)(q+2)}W^{(2)}_{(p-q)q}(\boldsymbol{r})\right). \tag{3.13}$$

Note that $D^{\delta\xi}_{00}$, $D^{\delta\xi}_{10}$ and $D^{\delta\xi}_{01}$ do not arise in the shape tensor as they do not survive second order differentiation. In the case of fibres with circular cross-sections $f(\theta)=1$ and it follows that $\hat{C}_{\delta\xi\alpha\beta}=0$ if $\delta+\xi+\alpha+\beta$ is odd. Since $\mathcal{A}^{(k)}_{\delta\xi}=O(\phi^{(\delta+\xi+2)/2})=W^{(k)}_{\delta\xi}$, equations (3.12)-(3.13) lead to the conclusion that $D^{\delta\xi}_{mn}=O(\phi^{(\delta+\xi-m-n+2)/2})$.

Equations (3.12) and (3.13) coupled with (3.4) give rise to an infinite homogeneous system of linear equations for the displacement gradient moments $W^{(k)}_{\delta\xi}$. A wave-like ansatz for these moments is now posed.

(b) Wave-like solutions

Define the variable $\boldsymbol{u}=\boldsymbol{p}-\boldsymbol{r}$ and noting (2.8), wseek plane wave type solutions of (3.4) of the form

$$W^{(k)}_{ij}(\boldsymbol{r}) = \hat{W}^{k}_{ij}\ell^{i+j+2}\exp(i\boldsymbol{\gamma}\cdot\boldsymbol{r}), \tag{3.14}$$

with $\boldsymbol{\gamma}(\Theta)=\varepsilon\gamma(\Theta)(\cos\Theta,\sin\Theta)$ being the non-dimensional effective wavenumber (scaled on q) in the direction of the angle subtended from the x_1 axis, Θ. Furthermore define

$$D^{\delta\xi}_{mn} = \ell^{\delta+\xi-m-n+2}\hat{D}^{\delta\xi}_{mn}. \tag{3.15}$$

Therefore, using (2.7), (3.7), (3.12), (3.13), (3.14) and (3.15) in (3.4) (recalling $k=1,2$) and again recalling (2.8),

$$\frac{\hat{W}^{(1)}_{\delta\xi}}{(1-m)} - \sum_{i,j,\alpha,\beta=0}^{\infty}\left(\hat{C}_{\delta\xi\alpha\beta}\left(\tau\phi^{\frac{1}{2}}\right)^{i+j+\alpha+\beta+2}\left\{\hat{W}^{(1)}_{ij}A[i+\alpha+2,j+\beta]\right.\right.$$
$$\left.\left. + \hat{W}^{(2)}_{ij}A[i+\alpha+1,j+\beta+1]\right\}\right) = \sum_{p=0}^{\mathcal{P}}\sum_{q=0}^{p+2}\left(\hat{D}^{\delta\xi}_{(p-q+2)q}\hat{W}^{(1)}_{(p-q)q} + \hat{D}^{\delta\xi}_{(p-q+1)(q+1)}\hat{W}^{(2)}_{(p-q)q}\right), \tag{3.16}$$

$$\frac{\hat{W}^{(2)}_{\delta\xi}}{(1-m)} - \sum_{i,j,\alpha,\beta=0}^{\infty}\left(\hat{C}_{\delta\xi\alpha\beta}\left(\tau\phi^{\frac{1}{2}}\right)^{i+j+\alpha+\beta+2}\left\{\hat{W}^{(1)}_{ij}A[i+\alpha+1,j+\beta+1]\right.\right.$$
$$\left.\left. + \hat{W}^{(2)}_{ij}A[i+\alpha,j+\beta+2]\right\}\right) = \sum_{p=0}^{\mathcal{P}}\sum_{q=0}^{p+2}\left(\hat{D}^{\delta\xi}_{(p-q+1)(q+1)}\hat{W}^{(1)}_{(p-q)q} + \hat{D}^{\delta\xi}_{(p-q)(q+2)}\hat{W}^{(2)}_{(p-q)q}\right) \tag{3.17}$$

where

$$A[m,n] = \sum_{\boldsymbol{u}\neq\boldsymbol{0}}\partial^{m}_{u_1}\partial^{n}_{u_2}G_{\varepsilon}(\boldsymbol{u})\exp(i\boldsymbol{\gamma}\cdot\boldsymbol{u}) \tag{3.18}$$

is a lattice sum, which shall now be discussed further.

(c) Lattice sums

First pick out the singular, non-integrable behaviour of the derivative of the Green's function in the lattice sum, as $|\boldsymbol{u}| \to 0$ which shall be defined as

$$S[m,n] = \lim_{|\boldsymbol{u}|\to 0} \partial_{u_1}^m \partial_{u_2}^n G_\varepsilon(\boldsymbol{u}),$$

Then for a given m, n, the infinite sums in (3.16) and (3.17) can be written in the form

$$A[m,n] = \sum_{\boldsymbol{u}\neq\boldsymbol{0}} \left[\left(\partial_{u_1}^m \partial_{u_2}^n G_\varepsilon(\boldsymbol{u}) - S[m,n]\right)\exp(i\boldsymbol{\gamma}\cdot\boldsymbol{u})\right] + L[m,n], \tag{3.19}$$

where

$$L[m,n] = \sum_{\boldsymbol{u}\neq\boldsymbol{0}} S[m,n]\exp(i\boldsymbol{\gamma}\cdot\boldsymbol{u}). \tag{3.20}$$

The first term of (3.19) can be turned into an integral in the same manner as in Sec. 3(a) of [17]. It transpires that when this step is applied, one if left with an integral that is $O(1)$ with respect to ε, multiplied by a factor $\varepsilon^{i+j+\alpha+\beta}$. Therefore the only term from this sum to integral step that contributes at $O(1)$ with respect to ε is the case when $i = j = \alpha = \beta = 0$.

Therefore, to $O(1)$ with respect to ε,

$$A[i+\alpha+p, j+\beta+q] = \begin{cases} I[p,q] + L[p,q] & \text{if } i=j=\alpha=\beta=0 \\ L[i+\alpha+p, j+\beta+q] & \text{otherwise,} \end{cases} \tag{3.21}$$

where $p + q = 2$ and

$$I[p,q] = \lim_{\varepsilon\to 0} \frac{1}{\mathcal{R}} \int_{-\infty}^{\infty}\int_{-\infty}^{\infty} \left(\partial_{u_1}^p \partial_{u_2}^q G_\varepsilon(\boldsymbol{u}) - S[m,n]\right)\exp(i\boldsymbol{\gamma}\cdot\boldsymbol{u}) d\boldsymbol{u}.$$

Taking $\Theta = 0$ and defining $\gamma(0) = \gamma_1$, so that the wavenumber vector is $\boldsymbol{\gamma} = \varepsilon(\gamma_1, 0)$ with γ_1 being the effective wavenumber in the x_1 direction it was shown in the appendices to [17], that (using the notation here)

$$I[2,0] = \frac{1}{\gamma_1^2 - 1} =: \Gamma(\gamma_1), \quad I[1,1] = I[0,2] = 0. \tag{3.22}$$

If one wishes to determine the effective wavenumber in the x_2 direction (seeking μ_2 instead of μ_1), it is straightforward to rotate the material by $\pi/2$. Performing this action leaves the above integrals unchanged, the wave is considered to propagate in the (new) x_1 direction, merely using notation γ_2 instead of γ_1 to indicate the wavenumber associated with the new material direction of propagation.

As regards $L[m,n]$ it should be noted that there are some further key results for that greatly simplify the process of obtaining the expressions for effective moduli. First, since the singular part of the Green's function contributing to the lattice sum satisfies Laplace's equation (except at the singular point, which is not important in the lattice summations), the lattice sums will satisfy

$$L[m+2,n] = -L[m,n+2] \quad \forall m,n \in \mathbb{Z}. \tag{3.23}$$

Furthermore, only cases where *both* m *and* n are even will give a non-zero $L[m,n]$. For example, consider the case of $L[1,2] = -L[3,0]$ due to (3.23). The associated $S[m,n]$ takes the form

$$\begin{aligned} -S[3,0] = &= -\frac{\partial^3}{\partial u_1^3}\left(\frac{1}{2\pi}\ln|\boldsymbol{u}|\right) \\ &= \frac{3u_1u_2^2 - u_1^3}{\pi|\boldsymbol{u}|^3}. \end{aligned}$$

When this is employed in the lattice sum (3.20), then in the limit as $\varepsilon \to 0$, due to the odd powers of u_1 in the numerator then when the summation over all nonzero $\boldsymbol{u}$ is made, all the terms where u_1 is positive will cancel with those where u_1 is negative, so that the lattice sum must be zero. This reasoning works equally well for all lattice sums whose indices total an odd number.

It is shown in Appendix B how the non-zero $L[m,n]$ can be straightforwardly determined.

(d) The asymptotic system in ϕ

Using (3.21) in (3.16) and (3.17) we find that the leading order (with respect to ε) system of equations is

$$\frac{\hat{W}^{(1)}_{\delta\xi}}{(1-m)} - \hat{C}_{\delta\xi 00}\beta^2\phi\hat{W}^{(1)}_{00}\Gamma(\gamma_1) - (1-m)\sum_{i,j,\alpha,\beta=0}^{\infty}\left(\hat{C}_{\delta\xi\alpha\beta}\left(\tau\phi^{\frac{1}{2}}\right)^{i+j+\alpha+\beta+2}\left\{\hat{W}^{(1)}_{ij}L[i+\alpha+2,j+\beta] + \hat{W}^{(2)}_{ij}L[i+\alpha+1,j+\beta+1]\right\}\right) = \sum_{p=0}^{\mathcal{P}}\sum_{q=0}^{p+2}\left(\hat{D}^{\delta\xi}_{(p-q+2)q}\hat{W}^{(1)}_{(p-q)q} + \hat{D}^{\delta\xi}_{(p-q+1)(q+1)}\hat{W}^{(2)}_{(p-q)q}\right), \tag{3.24}$$

$$\frac{\hat{W}^{(2)}_{\delta\xi}}{(1-m)} - \sum_{i,j,\alpha,\beta=0}^{\infty}\left(\hat{C}_{\delta\xi\alpha\beta}\left(\tau\phi^{\frac{1}{2}}\right)^{i+j+\alpha+\beta+2}\left\{\hat{W}^{(1)}_{ij}L[i+\alpha+1,j+\beta+1] + \hat{W}^{(2)}_{ij}L[i+\alpha,j+\beta+2]\right\}\right) = \sum_{p=0}^{\mathcal{P}}\sum_{q=0}^{p+2}\left(\hat{D}^{\delta\xi}_{(p-q+1)(q+1)}\hat{W}^{(1)}_{(p-q)q} + \hat{D}^{\delta\xi}_{(p-q)(q+2)}\hat{W}^{(2)}_{(p-q)q}\right). \tag{3.25}$$

This is an eigenvalue problem with eigenvalues γ_1 and associated eigenvectors comprising the moments $\hat{W}^{(k)}_{\delta\xi}$, noting that γ_1 appears only in the term $\Gamma(\gamma_1)$. In order to make progress take expansions in the volume fraction parameter

$$\hat{W}^{(1)}_{\delta\xi} = u^0_{\delta\xi} + u^1_{\delta\xi}\phi + u^2_{\delta\xi}\phi^2 + \ldots, \tag{3.26}$$

$$\hat{W}^{(2)}_{\delta\xi} = v^0_{\delta\xi} + v^1_{\delta\xi}\phi + v^2_{\delta\xi}\phi^2 + \ldots, \tag{3.27}$$

$$\Gamma(\gamma_1) = \frac{a_{-1}}{\phi} + a_0 + a_1\phi + a_2\phi^2 + \ldots, \tag{3.28}$$

where the form for Γ is motivated by (3.22) and the fact that $\gamma_1 \to 1$ as $\phi \to 0$.

Note the ϕ (ℓ) scaling of the wavetype solutions (3.14), so moments whose indices total an odd number will have a fractional leading order in ϕ. For instance, $W^{(k)}_{10}(\boldsymbol{r}) = O\left(\phi^{\frac{3}{2}}\right)$. This would suggest that, in general, powers of $\phi^{\frac{1}{2}}$ should be included in (3.26) to (3.28). However, restricting attention to shapes featuring a rotational symmetry of π, henceforth referred to as *centrally symmetric* shapes, then by observing the properties of the integrals in Appendix A it can be shown that such terms are not required. Proof of this is given in Appendix C, and the remainder of the methodology shall be discussed in the context of this restriction to central symmetry.

Given the scalings involved, using (3.22) and $\gamma_1^2 = 1/\mu_1^*$, (3.28) gives

$$\mu_1^* = \frac{a_{-1} + a_0\phi + a_1\phi^2 + a_2\phi^3 + \ldots}{a_{-1} + (1+a_0)\phi + a_1\phi^2 + a_2\phi^3 + \ldots} \tag{3.29}$$

The concern of the next section is the determination of the coefficients a_j from the linear system.

4. Determining explicit forms for the effective properties

Equation (3.29) provides an explicit form for the effective shear modulus, as a rational function in ϕ, providing the coefficients a_j can be determined. Note that the approximation provided in [17] was exactly this with both numerator and denominator truncated at $O(\phi)$. Here the objective is to determine higher order coefficients for a variety of fibre cross-sections.

There is a straightforward algorithmic mechanism for determining the coefficients a_j. Hereonin the term "$(\delta\xi)$ equations" shall refer to (3.24) and (3.25) for fixed δ and ξ. Start by noting

that expressions for the a_j coefficients arise by considering the first (00) equation, (3.24), using the expansions (3.26)-(3.28) and equating each order in ϕ of the resulting equation. In order to determine all coefficients up to a_N, say, the first (00) equation must be considered up to order ϕ^{N+1}. Each order provides an expression for a coefficient a_j in terms of the eigenvector components u^j_{00}, lattice sums, coefficients of the shape tensors and possibly components from other moments $u^j_{\delta\xi}$ and $v^j_{\delta\xi}$. By observing which terms from the displacement gradient moments appear in this highest order equation, one can then see which truncation with respect to the choices of indices $(\delta\xi)$ needs to be made and hence which additional $(\delta\xi)$ equations need to be considered in order to solve the linear system for the required terms $u^j_{\delta\xi}$ and $v^j_{\delta\xi}$ and hence subsequently a_i. The following examples illustrate the implementation of this scheme.

(a) Example: Elliptical cylindrical fibres

Consider elliptical cylindrical fibres of arbitrary aspect ratio ϵ, which is the the semi axis length in the x_2 direction, b, divided by the semi axis length in the x_1 direction a. At $O(1)$, noting that $\hat{C}_{0000}\tau^2 = 1$, where we recall that τ is defined for a given shape in (2.7) and writing without loss of generality that $u^0_{00} = 1$, it is determined that

$$a_{-1} = \frac{a + mb}{(1-m)(a+b)}. \tag{4.1}$$

Note also that the second (00) equation yields $v^0_{00} = 0$. The $O(\phi)$ terms give (upon using the properties of the lattice sum)

$$\frac{u^1_{00}}{(1-m)} = a_{-1}u^1_{00} + a_0 u^0_{00} + u^0_{00}L[2,0] + \frac{bu^1_{00}}{a+b},$$

and after using (4.1) and $v^0_{00} = 0$ this gives

$$0 = (L[2,0] + a_0)u^0_{00} \quad \Longrightarrow a_0 = -L[2,0], \tag{4.2}$$

while the second (00) equation to the same order simply gives $v^1_{00} = 0$.

Continuing in this vein, (3.29) takes the form

$$\mu^*_j = \frac{p_{0j} + \frac{1}{2}(S_j - 1)\phi - p_{2j}C_{4j}\phi^2 - p_{3j}C_{6j}\phi^3 - p_{4j}C^2_{4j}\phi^4 + \ldots}{p_{0j} + \frac{1}{2}(S_j + 1)\phi - p_{2j}C_{4j}\phi^2 - p_{3j}C_{6j}\phi^3 - p_{4j}C^2_{4j}\phi^4 + \ldots}, \tag{4.3}$$

where $L[2,0] = -L[0,2] = -(S_j - 1)/2$, C_{4j} depend upon the fourth order lattice sum and the p_{ij} coefficients are polynomial quotients in m, dependent on aspect ratio. Their forms are too lengthy to be given here but can straightforwardly be derived by implementing the algorithm above. As one should expect through checking for consistency with other leading order approximations

$$p_{01} = a_{-1} = \frac{a + mb}{(1-m)(a+b)}, \quad p_{02} = \frac{b + ma}{(1-m)(a+b)}. \tag{4.4}$$

For the specific case of fibres arranged on a square lattice, one finds that

$$\mu^*_j = \frac{p_{0j} - \frac{1}{2}\phi - p_{2j}C_{4j}\phi^2 - p_{4j}C^2_{4j}\phi^4 + \ldots}{p_{0j} + \frac{1}{2}\phi - p_{2j}C_{4j}\phi^2 - p_{4j}C^2_{4j}\phi^4 + \ldots}. \tag{4.5}$$

Details of how higher order terms are derived will be given explicitly in the next section for the case of circular cross-sections.

(b) Example: Circular cylindrical fibres

To illustrate specific details of the derivation of higher order terms, consider the circular cross-sectional case, $a = b = 1$ for which the details of the last section are clearly valid. Consider the first (00) equation to $O(\phi^2)$. After evaluating the $\hat{C}_{00\alpha\beta}$ coefficients in the quadruple sum, using the relations (3.23) and the rule involving odd indices within the lattice sum, in addition to the result

from the previous section that $v^1_{00}=0$ and the forms (4.1) and (4.2) for a_{-1} and a_0, the equation reduces to

$$0=a_1u^0_{00}+\frac{1}{\pi}(u^0_{20}-u^0_{02}-v^0_{11})L[4,0]. \tag{4.6}$$

This illustrates how higher order moment terms arise, in this case u^0_{20}, u^0_{02} and v^0_{11}, and therefore motivates which equations need to be studied subsequently. In this case, it means that the (11), (20) and (02) equations must be considered at leading order with respect to ϕ in order to obtain a_1. Using the naming convention that the collective set of (ij) equations where $i+j=n$ shall be referred to as the order n equations, here the interest is therefore in the order 2 equations.

It transpires that these order 2 equations partition into two non-trivial decoupled sub-systems: the first (20) and (02) equations and the second (11) equation form a system in $\hat{W}^{(1)}_{20}$, $\hat{W}^{(1)}_{02}$ and $\hat{W}^{(2)}_{11}$, while the second (20) and (02) equations and the first (11) equation form a system in $\hat{W}^{(2)}_{20}$, $\hat{W}^{(2)}_{02}$ and $\hat{W}^{(1)}_{11}$. The latter subsystem is homogeneous with respect to the leading order coefficients of the moments featured, while (4.6) illustrates how the former contributes to the process of obtaining a_1. Hence, making use of (4.1) for $a=b=1$ and all other solutions from prior orders of ϕ, the leading order equations of the former sub-system take the form

$$\begin{aligned}
0&=\frac{1}{16}u^0_{00}\left(\frac{1+m}{1-m}-1\right)+\frac{1}{8}u^1_{02}+\left(\frac{7}{8}-\frac{1}{1-m}\right)u^1_{20}+\frac{1}{8}v^1_{11},\\
0&=\frac{1}{16}u^0_{00}\left(\frac{1+m}{1-m}+1\right)+\left(\frac{1}{8}-\frac{1}{1-m}\right)u^1_{02}-\frac{1}{8}u^1_{20}+\frac{1}{8}v^1_{11},\\
0&=-\frac{1}{8}u^0_{00}+\frac{1}{2}u^1_{02}+\frac{1}{2}u^1_{20}+\left(\frac{1}{2}-\frac{1}{1-m}\right)v^1_{11}.
\end{aligned}$$

Solving these equations gives

$$u^1_{20}=u^1_{02}=\frac{u^0_{00}}{8},\quad v^1_{11}=0,$$

and hence (4.6) gives $a_1=0$.

Proceeding to general orders, with the aid of a symbolic package such as Mathematica, for general parallelogram lattices, results for circular cylindrical fibres take the form

$$\mu^*_j=\frac{1+(S_j-1)\mathcal{M}\phi-\frac{\mathcal{M}^2C^2_{4j}}{3\pi^2}\phi^4-\frac{\mathcal{M}^2C^2_{6j}}{720\pi^4}\phi^6-\frac{\mathcal{M}^3C^2_{4j}C_{6j}}{18\pi^4}\phi^7-\frac{\mathcal{M}^2C^2_{8j}}{\pi^6}\phi^8+\ldots}{1+(S_j+1)\mathcal{M}\phi-\frac{\mathcal{M}^2C^2_{4j}}{3\pi^2}\phi^4-\frac{\mathcal{M}^2C^2_{6j}}{720\pi^4}\phi^6-\frac{\mathcal{M}^3C^2_{4j}C_{6j}}{18\pi^4}\phi^7-\frac{\mathcal{M}^2C^2_{8j}}{\pi^6}\phi^8+\ldots}, \tag{4.7}$$

where $\mathcal{M}=(1-m)/(1+m)$. Note that the sixth order lattice sum is zero for square lattices, hence $C_{6j}=0$ which is why order ϕ^6 and ϕ^7 terms appear in the general case and not the square lattice case.

In the special case when circular cylindrical fibres on a square lattice, expressions for the effective shear moduli take the form

$$\mu^*_j=\frac{1-\mathcal{M}\phi-\frac{\mathcal{M}^2C^2_{4j}}{3\pi^2}\phi^4-\frac{\mathcal{M}^2C^2_{8j}}{\pi^6}\phi^8+\ldots}{1+\mathcal{M}\phi-\frac{\mathcal{M}^2C^2_{4j}}{3\pi^2}\phi^4-\frac{\mathcal{M}^2C^2_{8j}}{\pi^6}\phi^8+\ldots} \tag{4.8}$$

This is consistent with the form of higher order terms outlined in the conclusions of [17].

(c) More general fibre cross-sections

Although rather lengthy, analytical forms for the effective shear moduli associated with general cross-sections *can* be obtained. The procedure above can be followed and certainly in a symbolic package such as Mathematica, forms can be derived. However such expressions are too lengthy and cumbersome in general to be provided here[1]. Importantly, for a given cross-sectional shape, using the above procedure, a rational function approximation for the effective properties as a

[1]The algorithm to derive explicit forms for rather general shapes will be provided in an online repository upon publication

function of ϕ can be derived and subsequently used to great utility. In the following section we discuss results obtained for shapes more general than elliptical and validate the scheme with the classical method of asymptotic homogenization (MAH). The argument for using the present scheme over the MAH (or other methods) is that this integral equation methodology can yield explicit forms, particularly when some aspects of the medium are fixed (e.g. square lattice, fixed m), of the effective moduli, retaining dependence on ϕ. Such forms can then be used with great rapidity in models without the need for recourse to finite element simulations as soon as one changes, for example the volume fraction, as is required in the MAH for general shapes, for example.

5. Results

The implementation of the above methodology is now described for a range of geometries in the case of a shear contrast of $m = 18.75$ (graphite fibres in epoxy). To fix ideas and since general cross-sections are of principal interest here, attention is restricted to the case of square lattices. Extension to other lattices is straightforward. Results derived using the methodology shall be compared with those obtained using the MAH [5]. It transpires that the effective antiplane shear modulus (when scaled on that of the host medium) as determined by the MAH can be written in the form (see Eqs. (3.25) and (3.26) of [5])

$$\mu_1^* = 1 + (m-1)(\phi + H_{11}), \quad \mu_2^* = 1 + (m-1)(\phi + H_{22}), \tag{5.1}$$

where the tensor components of $\mathbf{H}$ may be described as follows

$$\boldsymbol{H} = \int_{V_{ab}} \nabla_{\boldsymbol{\xi}} \boldsymbol{N} d\boldsymbol{\xi} = \int_{\partial V_{ab}} \boldsymbol{N} \cdot \boldsymbol{n} ds = \begin{bmatrix} H_{11} & H_{12} \\ H_{21} & H_{22} \end{bmatrix}. \tag{5.2}$$

Here $\boldsymbol{n}$ is the outer unit normal to the fibre boundary ∂V_{ab}, $\boldsymbol{\xi}$ is the short lengthscale of the problem and $\boldsymbol{N} = (N_1, N_2)$ is the solution to the associated *cell problem*. In the case of square lattices as considered for these results, $H_{12} = H_{21} = 0$, and if the fibre cross section has a rotational symmetry of $\pi/2$, $H_{11} = H_{22}$ and thus $\mu_1^* = \mu_2^*$. Generally for fibres of non-circular cross-section, the finite element method is employed to solve the cell problem. Indeed here we use COMSOL multiphysics to solve the cell problem for antiplane shear. We compare the methods by plotting the components H_{11} and H_{22} of the H-tensor. It shall be shown that this is a very sensitive measure of the accuracy of the integral equation scheme and generally speaking, it provides excellent accuracy even at extremely high volume fractions, for relatively low order approximations of the rational function form.

(a) Circular Cylindrical Fibres

Consider circular fibres of radius r. Figure 2 compares results for $H_{11}(r)$ as obtained from (4.8) when truncated to different orders of ϕ (so for example order 4 refers to the estimate given by (4.8) when terms up to order ϕ^4 are included on the top and bottom) to those from using the MAH. Results are plotted against the radius r of the circular cylindrical fibre inside the cell and related to the volume fraction ϕ via equation (2.7) for $f(\theta) = 1$ and $\mathcal{R} = 1$. Results for the MAH when utilising the multipole method [5] and the finite element method (FEM) are both plotted to illustrate that the FEM remains consistent with the multipole method. Agreement between the MAH and the present integral equation method (IEM) estimates is, in general, excellent until the radius begins to approach 0.5, referred to as the packing limit. In this limit, fibres begin to be in contact with each other and clearly other effects become important. The right hand plot of Figure 2 focuses on values of the radius close to this packing limit. Thus it appears that the highest order IEM employed here (order 12) estimate begins to deviate from the MAH estimate around 0.48, although this is deviation when studying the tensor components of $\mathbf{H}$. Generally the impact of this deviation on *effective properties* is weaker as will be seen shortly.

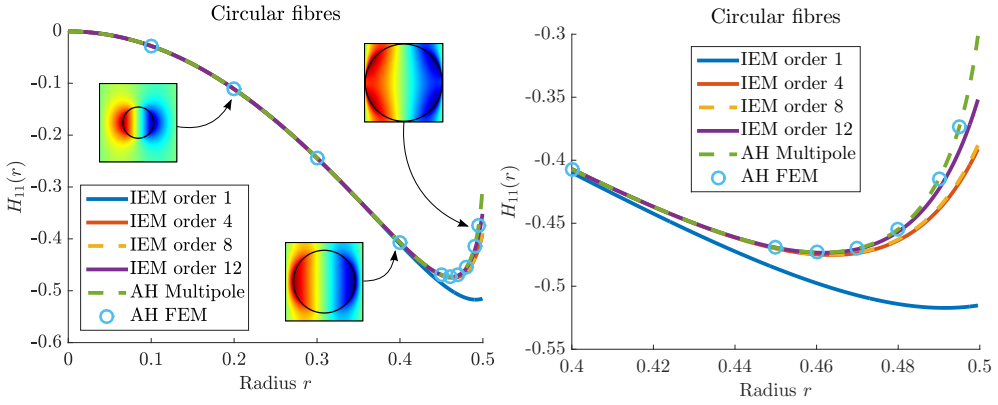

Figure 2: Plot of $H_{11}(r)$ for $m = 18.75$ when circular fibres are arranged on a square lattice, with associated solutions of the cell problem from the MAH inset (left) and a close-up for high radii (right).

(b) Elliptical Cylindrical Fibres

Figure 3 illustrates results obtained in the case of elliptical fibres with aspect ratio (major axis divided by minor axis) of $\epsilon = 2$ and here r is the major axis. As the left hand plot illustrates, agreement is excellent in general and it is only near the packing limit where the IEM and MAH results show any deviation. The right hand plot therefore magnifies this region.

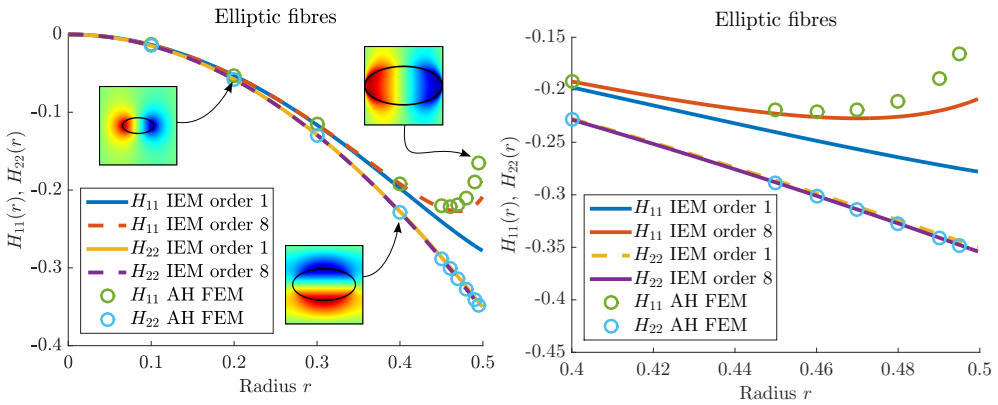

Figure 3: Plot of $H_{11}(r)$ and $H_{22}(r)$, where r is the major axis of the ellipse, for $m = 18.75$ when elliptical fibres of aspect ratio 2 are arranged on a square lattice, with associated solutions of the cell problem from the MAH inset (left) and a close-up for high radii (right).

One interesting aspect of these results comes from examining H_{22}, the component associated with μ_2. Here, the leading order IEM solution is in excellent agreement with the MAH results even at leading order, with the addition of terms up to order ϕ^8 only slightly increasing the accuracy close to the packing limit when the major axis $r = 0.5$. Contrast this with the H_{11} results; here the leading order IEM solution begins to behave significantly differently from the MAH solution close to $r = 0.4$. The IEM solution requires the addition of higher order terms to replicate the upturn that the MAH result experiences up to the packing limit. Even when including terms up to order

ϕ^8, the IEM cannot replicate this upturn precisely and the gradient of the result from $r = 0.45$ onwards does not quite match the MAH result in this region. Of course, this assumes that MAH is correct and one cannot be entirely sure that close to the packing limit that this is the case in terms of effective properties since other effects come into play.

The above effect should be expected of course, as the geometry of the composite is such that the major axis of the ellipse is in line with the x_1 coordinate. Consequently when close to the packing limit $r = 0.5$, while the inclusions within the composite will be close to/at the point of contact in the x_1 direction (i.e. a fibre from one cell will be close to touching the fibres in the left and right neighbouring cells), there will still be a significant distance between fibres in neighbouring cells in the x_2 direction (cells directly above or below a cell). This essentially causes the problem to be, in a sense, significantly more dilute with respect to the x_2 direction than to the x_1 direction, since there will still be significant portions of the composite comprised of the host phase in the x_2 direction even when the fibres are near the point of contact. Therefore it makes sense that IEM is able to produce high accuracy results for H_{22} and hence μ_2^* even without the addition of higher order terms, since the method shows very strong agreement with results from other known methods in dilute cases (as all of the results so far for low values of the radius/major axis illustrate).

(c) Results For Other Fibre Cross Sections

As already outlined, this method is designed to work with fibres of rather general cross section. Having established promising results for fibres of elliptical cross section, it would be of interest to examine how successful the method is with more complicated cross sections. Polygons appear to be one class of shapes which are an ideal successor to ellipses when considering additional geometrical complexities within the problem.

The left hand plot of Figure 4 examine the results for $H_{11}(r)$ and $H_{22}(r)$ in the case of rectangular shaped fibres with aspect ratio 2 and where r is the long axis of the rectangle. In addition, the right hand plot of Figure 4 shows the results for the actual effective shear modulus μ_1^* for all three fibre shapes considered thus far, when plotted against volume fraction, as opposed to fibre “radius". Figure 5 plots both effective shear moduli against fibre “radius". As well as returning the results to the context of the effective properties sought, these plots again help illustrate the extra sensitivity the $\mathbf{H}-$tensor components exhibit, i.e. in general even for quite small order approximations the IEM appears to provide exceptional predictions of the effective shear moduli, even up to extremely high volume fractions.

Naturally, as the rectangular cross-section features the same aspect ratio as the ellipse considered earlier, this composite experiences a similar phenomenon regarding the accuracy of results for H_{22} (and through this μ_2^*) as compared with those for H_{11} (and thus μ_1^*). In this instance, the method is able to replicate the upturn behaviour more accurately as compared to the elliptical case, with the leading order solution seeing its gradient flatten towards the very end of the plot and the order ϕ^6 solution replicating the upturn of the MAH result almost exactly (as opposed to the elliptical case, where even at order ϕ^8 the IEM could not fully produce an upturn as steep as required). The geometry of the rectangle is a large factor in this behaviour, as when two rectangles reach the point of contact ($r = 0.5$), the entirety of the left and right hand edges will be in contact with each other, as opposed to two ellipses, which will only be in contact with each other at one point. This means that as the size of inclusions reaches the packing limit, the regions close to the left and right hand edges of the cell will contain a much smaller proportion of the host material when the fibre cross sections are rectangles as opposed to ellipses, and the geometry of these regions of host material will also be much simpler for rectangles.

Figure 6 shows a plot of results for fibres of hexagonal shaped cross section in the context of the cell problem, with Figure 7 plotting the actual effective properties. Once again, there is extremely good agreement between the two methods.

As expected, since this hexagon features edges parallel to the left and right hand cell boundaries, the IEM results replicate the results for H_{11} to a greater accuracy than those of H_{22}. However, it is only in a region very close to the packing limit that the IEM results for H_{22} begin

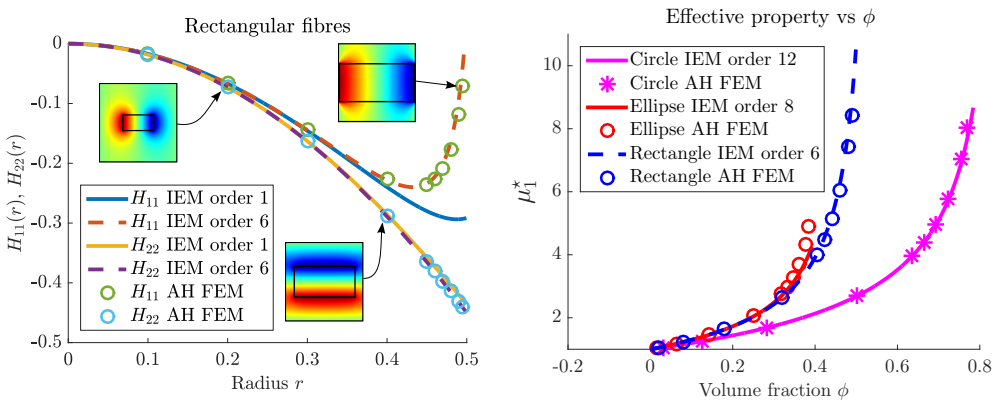

Figure 4: Plot of $H_{11}(r)$ and $H_{22}(r)$ for the situation when for $m = 18.75$ and rectangular fibres of aspect ratio 2 are arranged on a square lattice, with associated solutions of the cell problem from the MAH inset (left) and a plot of the effective property μ_1^* versus volume fraction for circular, rectangular and elliptical fibre cross-sections (right).

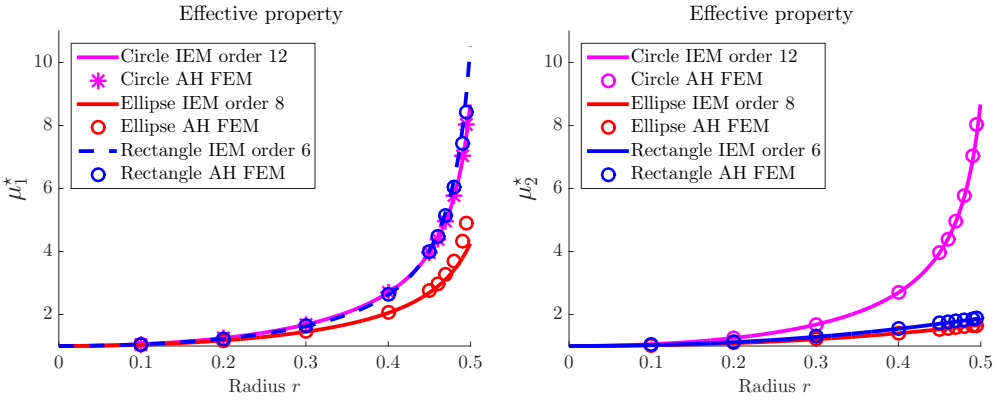

Figure 5: Plot of the effective antiplane shear moduli μ_1^* (left) and μ_2^* (right) versus fibre "radius" for the situation when circular, elliptical and rectangular fibres are arranged on a square lattice, $m = 18.75$.

to significantly differ from the MAH results, in failing to fully replicate the upturn at the very end of the MAH plot.

The so called "radius" parameter which the results are plotted against is the parameter which governs the area of the polygon within the unit cell. It comes from considering the radial distance from the centre of the polygon to its outer edge as a function of the polar angle θ. Indeed, if one has a two dimensional shape governed by a function $f(\theta)$ multiplied by a constant r, where the function f is designed to have a minimum of 1 which occurs at the point $\theta = 0$, so that r may be considered the minimum distance of the shape from its centre, then the area A can be written as

$$A = \frac{r^2}{2} \int_0^{2\pi} f^2(\theta) d\theta.$$

This area can then be used in place of the volume fraction, just as the volume fraction of elliptical fibres could be represented by the equation for the area of the ellipse in terms of its minor axis.

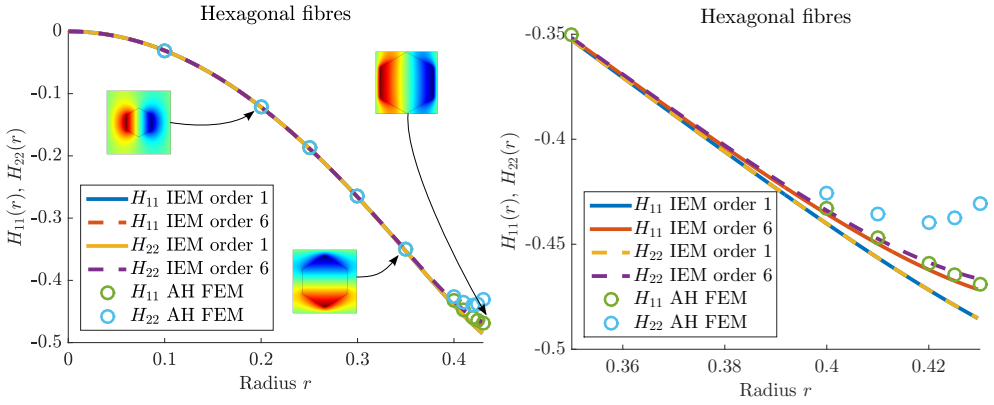

Figure 6: Plot of $H_{11}(r)$ and $H_{22}(r)$ for $m = 18.75$ when hexagonal fibres are arranged on a square lattice, with associated solutions of the cell problem from the MAH inset (left) and a close-up for high radii (right).

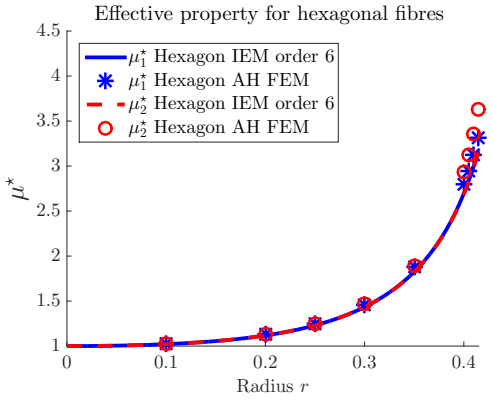

Figure 7: Plot of effective antiplane shear moduli μ_1^* and μ_2^* for $m = 18.75$ when hexagonal shaped fibres are arranged on a square lattice.

The f functions for polygons are actually a sub class of a more general shape function of the form

$$f(\theta) = \left(\left| \frac{1}{a} \cos\left(\frac{m}{4}\theta\right) \right|^{n_2} + \left| \frac{1}{b} \sin\left(\frac{m}{4}\theta\right) \right|^{n_3} \right)^{-1/n_1}.$$

Further detail on this so called “superellipse" function can be found in work by Gielis [23]. For reference, in the case of the hexagon, a and b are 1, $n_1 = 100$, $m = 6$ and $n_2 = n_3 = 62$. For the rectangle, $a = 2$, $b = 1$, $m = 4$ and $n_1 = n_2 = n_3 = 200$.

6. Conclusion

New, explicit expressions for the effective properties of inhomogeneous media have been derived in the case of the scalar problem associated with periodic two-dimensional fibre reinforced composites. Results are broad in applicability due to the form, and can therefore be applied to the case of antiplane shear, thermal conductivity, etc. as has been described. Of specific interest is that the fibres in question can be of rather general cross-section and results obtained have been

validated successfully with the classical method of asymptotic homogenization. The advantage of the present scheme is that the forms can be used for general volume fractions without recourse to computational methods, such as finite element schemes. The method is designed with general fibre cross section shapes in mind, but in the special case of centrally symmetric shapes results such as (4.3) and (4.7) may be obtained. Extensions to the case of full elastodynamics and three-dimensional scenarios for both the potential problem and elastodynamics are currently underway.

Acknowledgements

Joyce is grateful to Thales Underwater Systems Ltd and EPSRC for funding via a CASE PhD studentship. Parnell acknowledges the Engineering and Physical Sciences Research Council for funding his research fellowship (EP/L018039/1) and Abrahams thanks the Royal Society for a Wolfson Research Merit award (2013-2018).

A. Two Dimensional J Tensor Expansion

Consider (3.10) with G_ε replaced by G_0 as defined in (2.6). Define the planar polar coordinate systems

$$\boldsymbol{x}-\boldsymbol{r}=\hat{\rho}(\cos\hat{\theta},\sin\hat{\theta}), \qquad\qquad \boldsymbol{y}-\boldsymbol{r}=\rho(\cos\theta,\sin\theta)$$

with $\rho,\hat{\rho}\geq 0$ and $0\leq\theta,\hat{\theta}<2\pi$. Also define the boundary of the cross-sectional shape as

$$\hat{\rho}=f(\hat{\theta})$$

where $f(\hat{\theta})\geq 1$ for all $\hat{\theta}$. Thus

$$J_{\delta\xi}(\boldsymbol{y})=\frac{1}{4\pi\delta!\xi!}\int_V \hat{\rho}^{\delta+\xi+1}\cos^\delta\hat{\theta}\sin^\xi\hat{\theta}\ln\left(\rho^2+\hat{\rho}^2-2\rho\hat{\rho}\cos(\theta-\hat{\theta})\right)\ d\hat{\rho}d\hat{\theta} \tag{A 1}$$

In general it is clearly not possible to obtain an analytical form for this and it must be evaluated numerically for any point $\boldsymbol{y}\in D$, hence the motivation for a Taylor style expansion to approximate such integrals.

Pose the expansion (3.11). In terms of the local coordinates this may be rewritten as

$$J_{\delta\xi}(\rho,\theta)=a_0^{\delta\xi}(\rho)+\sum_{n=1}^{\mathcal{P}+2}a_n^{\delta\xi}(\rho)\cos(n\theta)+b_n^{\delta\xi}(\rho)\sin(n\theta), \tag{A 2}$$

where the a and b functions depend on the D coefficients from (3.11) (best found in a symbolic package such as mathematica) so that for example (with superscripts omitted for convenience)

$$a_0(\rho)=D_{0,0}+\frac{1}{4}\rho^2(D_{2,0}+D_{0,2})+\frac{1}{64}\rho^4(D_{40}+2D_{22}+D_{04})+\ldots$$

This yields an ideal situation for isolating the coefficients appearing in the a and b functions (and hence obtaining conditions they must adhear to) by using orthogonality of trigonometric functions. As such introduce the operators $\mathcal{C}_m$ and $\mathcal{S}_m$ as those which multiply by $\alpha_m\cos(m\theta)$ and $\alpha_m\sin(m\theta)$ and then integrate over $\theta\in[0,2\pi)$ where

$$\alpha_m=\begin{cases}\frac{1}{2\pi}, & m=0,\\ \frac{1}{\pi}, & m\geq 1.\end{cases}$$

Therefore, applying these operators to (A 1) = (A 2) and setting $\rho = 1$,

$$a_0^{\delta\xi}(1) = \frac{1}{8\pi^2\delta!\xi!}\int_D \hat{\rho}^{\delta+\xi+1}\cos^\delta\hat{\theta}\sin^\xi\hat{\theta}C_0(\hat{\rho},\hat{\theta})\ \ d\hat{\rho}d\hat{\theta}, \tag{A 3}$$

$$a_m^{\delta\xi}(1) = \frac{1}{4\pi^2\delta!\xi!}\int_D \hat{\rho}^{\delta+\xi+1}\cos^\delta\hat{\theta}\sin^\xi\hat{\theta}C_m(\hat{\rho},\hat{\theta})\ \ d\hat{\rho}d\hat{\theta}, \tag{A 4}$$

$$b_m^{\delta\xi}(1) = \frac{1}{4\pi^2\delta!\xi!}\int_D \hat{\rho}^{\delta+\xi+1}\cos^\delta\hat{\theta}\sin^\xi\hat{\theta}S_m(\hat{\rho},\hat{\theta})\ \ d\hat{\rho}d\hat{\theta} \tag{A 5}$$

where

$$C_m(\hat{\rho},\hat{\theta}) = \int_0^{2\pi}\cos(m\theta)\ln\left(\hat{\rho}^2+1-2\hat{\rho}\cos(\theta-\hat{\theta})\right)\ \ d\theta, \tag{A 6}$$

$$S_m(\hat{\rho},\hat{\theta}) = \int_0^{2\pi}\sin(m\theta)\ln\left(\hat{\rho}^2+1-2\hat{\rho}\cos(\theta-\hat{\theta})\right)\ \ d\theta. \tag{A 7}$$

Note that $f(\hat{\theta}) \geq 1$. By performing a change of variables, $\psi = \theta - \hat{\theta}$, employing double angle formulae for the trigonometric functions and using the following identities (Gradshteyn and Ryzhik [24]),

$$\int_0^{2\pi}\ln\left(\hat{\rho}^2+1-2\hat{\rho}\cos\psi\right)\ \ d\psi = \begin{cases} 0, & \hat{\rho}^2<1, \\ 2\pi\ln\hat{\rho}^2, & \hat{\rho}^2>1. \end{cases}$$

$$\int_0^{2\pi}\cos(m\psi)\ln\left(\hat{\rho}^2+1-2\hat{\rho}\cos\psi\right)\ \ d\psi = \begin{cases} -\frac{2\pi}{m}\hat{\rho}^m, & \hat{\rho}^2<1, \\ -\frac{2\pi}{m}\hat{\rho}^{-m}, & \hat{\rho}^2>1. \end{cases}$$

where $m \geq 1$ in the latter, one finds

$$\begin{aligned} a_0^{\delta\xi}(1) &= \frac{1}{2\pi\delta!\xi!(\delta+\xi+2)^2}\int_0^{2\pi}\cos^\delta\hat{\theta}\sin^\xi\hat{\theta}\left[\left(f(\hat{\theta})\right)^{\delta+\xi+2}\left((\delta+\xi+2)\ln f(\hat{\theta})-1\right)+1)\right]\ \ d\hat{\theta} \\ &= \mathcal{A}_0^{\delta\xi} \end{aligned}$$

where integration by parts in order was used for the ζ integration and a different notation has been associated with this integral form so that it may be referred to later. Also

$$a_m^{\delta\xi}(1) = -\frac{1}{2\pi\delta!\xi!}\int_0^{2\pi}\cos^\delta\hat{\theta}\sin^\xi\hat{\theta}\cos(m\hat{\theta})\left[\frac{1}{\delta+\xi+m+2}+\mathcal{J}_{\delta+\xi-m}(\hat{\theta})\right]\ \ d\hat{\theta} = A_m^{\delta\xi} \tag{A 8}$$

where

$$\mathcal{J}_{\delta+\xi-m}(\hat{\theta}) = \begin{cases} \ln\left(f(\hat{\theta})\right), & \delta+\xi-m=-2, \\ \dfrac{\left(f(\hat{\theta})\right)^{\delta+\xi-m+2}-1}{\delta+\xi-m+2}, & \text{otherwise} \end{cases}$$

and similarly

$$b_m^{\delta\xi}(1) = -\frac{1}{2\pi\delta!\xi!}\int_0^{2\pi}\cos^\delta\hat{\theta}\sin^\xi\hat{\theta}\sin(m\hat{\theta})\left[\frac{1}{\delta+\xi+m+2}+\mathcal{J}_{\delta+\xi-m}(\hat{\theta})\right]\ \ d\hat{\theta} = B_m^{\delta\xi}.$$

However, more conditions are needed in order to close the system. These are obtained by applying the Laplacian operator to (3.10) and (3.11), exploiting that $\nabla^2 G = \delta(\boldsymbol{y}-\boldsymbol{x})$,

$$\begin{aligned} \frac{(y_1-r_1)^\delta(y_2-r_2)^\xi}{\delta!\xi!} = \sum_{n=2:p+q=2}^{N}\frac{D_{pq}^{\delta\xi}}{p!q!}\Big(&p(p-1)(y_1-r_1)^{p-2}(y_2-r_2)^q \\ &+q(q-1)(y_1-r_1)^p(y_2-r_2)^{q-2}\Big). \end{aligned}$$

Comparing coefficients of $(y_1 - r_1)^i (y_2 - r_2)^j$ provides equations linking the coefficients $D^{\delta\xi}_{pq}$. Some thought leads to the conclusion that for $p, q \geq 2$

$$D^{\delta\xi}_{(p+2)q} + D^{\delta\xi}_{p(q+2)} = \delta_{p\delta}\delta_{q\xi}.$$

(a) Linear system

Now employ the equations relating a_m, b_m and D_{pq} and equate these to the integral forms just developed above, so that e.g.

$$a^{\delta\xi}_0(1) = D^{\delta\xi}_{00} + \frac{1}{4}(D^{\delta\xi}_{20} + D^{\delta\xi}_{02}) + \frac{1}{64}(D^{\delta\xi}_{40} + 2D^{\delta\xi}_{22} + D^{\delta\xi}_{04}) + \ldots = A^{\delta\xi}_0$$

In fact upon employing the Laplacian conditions the full linear system for the unknowns may be written in the diagonal form

$$\mathbf{ID} = \mathbf{F} + \mathbf{R}$$

where

$$\mathbf{D} = [D_{00} \;\; D_{10} \;\; D_{01} \;\; D_{20} \;\; D_{11} \;\; D_{30} \;\; D_{21} \;\; D_{40} \;\; D_{31} \ldots]^T$$

$$\mathbf{F} = [A_0 \;\; A_1 \;\; B_1 \;\; A_2 \;\; B_2 \;\; A_3 \;\; B_3 \;\; A_4 \;\; B_4 \ldots]^T$$

and the vector $\mathbf{R}$ is essentially a sparse vector including some constants that arise due to the Laplacian simplification in the LHS. The difficulty is that it depends on the choice of $\delta\xi$ and on the truncation of the system.

The following examples are given due to their relevance to the example systems in Section (4).

(i) Elliptical Fibre Second Order Case: $\mathcal{P} = 0$, $\delta = \xi = 0$

For this case, only $J_{00}(\rho, \theta)$ is sought as a polynomial expansion of the form

$$J_{00} = \hat{D}^{00}_{00} + D^{00}_{10}(\tilde{y}_1 - \tilde{r}_1) + D^{00}_{01}(\tilde{y}_2 - \tilde{r}_2) + \frac{D^{00}_{20}}{2}(\tilde{y}_1 - \tilde{r}_1)^2 + \frac{D^{00}_{02}}{2}(\tilde{y}_2 - \tilde{r}_2)^2, \tag{A 5}$$

The above expressions clarify better why $\mathcal{P} = 0$ is referred to as the second order case: the sum of the lower indices of the D constants never exceed 2.

In this case, the only non-trivial coefficients that have an influence on the shape tensor term are

$$D^{00}_{20} = \frac{b}{(a+b)}, \quad D^{00}_{02} = \frac{a}{(a+b)},$$

so, using (3.12) and (3.13), the shape tensor for this system has the form

$$\hat{\mathcal{A}}^{(1)}_{00} = -\frac{b}{(a+b)}\hat{W}^{(1)}_{00}, \quad \hat{\mathcal{A}}^{(2)}_{00} = -\frac{a}{(a+b)}\hat{W}^{(2)}_{00}. \tag{A 4}$$

(ii) Circular Fibre Fourth Order Case Example: $\mathcal{P} = 2$, $\delta = 2, \xi = 0$

Note that in order to fully consider the equations (3.24) and (3.25) to fourth order the cases $\delta = \xi = 1$ and $\delta = 0, \xi = 2$ must also be considered. The case $\delta = 2, \xi = 0$ has been chosen merely as an example to illustrate how the system for the shape tensor works at this order.

In this instance, the shape tensor may be written as

$$\hat{\mathcal{A}}^{(1)}_{20} = \frac{1}{16}\hat{W}^{(1)}_{00} - \frac{1}{8}\hat{W}^{(1)}_{02} - \frac{7}{8}\hat{W}^{(1)}_{20} - \frac{1}{8}\hat{W}^{(2)}_{11},$$

$$\hat{\mathcal{A}}^{(2)}_{20} = -\frac{1}{16}\hat{W}^{(2)}_{00} + \frac{1}{8}\hat{W}^{(2)}_{02} - \frac{1}{8}\hat{W}^{(2)}_{20} - \frac{1}{8}\hat{W}^{(1)}_{11}.$$

The fact that this shape tensor depends on displacement gradient moments for $\delta = \xi = 1$ and $\delta = 0$, $\xi = 2$ illustrates why those choices for δ and ξ must also be considered in order to fully establish this fourth order problem.

B. Lattice Sums

As (4.2) illustrates, the coefficients of $\Gamma(\gamma_1)$ will in general depend upon the lattice sums $L[m,n]$. While it has already been shown that these sum to zero when either n, m or both n and m are odd, and that many sums are equivalent to each other through the Helmholtz identity (3.23), it still remains to evaluate the non-trivial sums (when n and m are even).

Recall from the definition (3.20) that

$$L[m,n] = \sum_{\boldsymbol{u}\neq\boldsymbol{0}} \exp(i\boldsymbol{\gamma}\cdot\boldsymbol{u}) S[m,n],$$

where $S[m,n]$ is the singular part of the of the Green's function differentiated m times with respect to u_1 and n times with respect to u_2. In the case of this problem, attention is restricted to parallelogram shaped lattices, which will in turn restrict the forms of $\boldsymbol{u}$ that appear in the summation. For ease of exposition, consider the further restriction of rectangular shaped lattices, so that the displacements to be summed over are of the form $\boldsymbol{u} = (Bu, v)$, where $B \geq 1$ is the aspect ratio and u and v are integers. Since the problem is also considered in the quasi-static limit $\varepsilon \ll 1$, Green's function takes the form G_0 as defined by (2.6), and the exponential term in (3.20) may be considered as tending to 1. An example is given to illustrate the procedure involved in evaluating such sums. Other sums are derived analogously.

(iii) Example: L[2,0] = -L[0,2]

The sum $L[2,0]$ (equivalent to $-L[0,2]$ by the Helmholtz identity) will involve the singular part of $\partial_{u_1}^2 G_0(\boldsymbol{u})$, which is of the form

$$S[2,0] = \frac{u_2^2 - u_1^2}{2\pi(u_1^2+u_2^2)^2}.$$

Upon inserting into the lattice sum definition and using the rectangular lattice restriction, this gives

$$L[2,0] = \frac{1}{2\pi} \sum_{(u,v)\neq(0,0)} \frac{v^2 - B^2u^2}{(B^2u^2+v^2)^2}.$$

By isolating the parts of the sum where $u=0$ and $v=0$ in turn, the above may be written as

$$L[2,0] = \frac{1}{\pi}\left(\sum_{v=1}^{\infty} \frac{1}{v^2} - \sum_{u=1}^{\infty} \frac{1}{B^2u^2} + 2\sum_{u=1}^{\infty}\sum_{v=1}^{\infty} \frac{v^2 - B^2u^2}{(B^2u^2+v^2)^2} \right)$$

where the sums from $-\infty$ to ∞ excluding 0 have been replaced by twice the sum from 1 to ∞ since the powers of u and v in the sum are all even. By first performing the summation with respect to v,

$$\begin{aligned} L[2,0] &= \frac{1}{\pi}\left(\frac{\pi^2}{6} - \sum_{u=1}^{\infty} \frac{1}{B^2u^2} + 2\sum_{u=1}^{\infty} \left[\frac{1}{2B^2u^2} - \frac{\pi^2}{2}\operatorname{cosech}^2(\pi Bu) \right] \right) \\ &= \frac{\pi}{6} - \pi \sum_{u=1}^{\infty} \operatorname{cosech}^2(\pi Bu), \end{aligned}$$

which defines this sum for rectangular lattices. Note that in the special case of square lattices, $B=1$, then performing the summation with respect to u yields

$$L[2,0] = 0.5.$$

In fact, it turns out that in the case of square lattices, even more of the lattice sums become trivial, as

$$L[2(2i+1),0] = 0 \quad \forall i \geq 1, \tag{A -7}$$

Thus via the Helmholtz identity, $L[m,n]$ will be zero for any even m and n whose total is an odd number multiplied by 2.

For example, in the general rectangular lattice case, $L[6,0]$ has the form

$$L[6,0]=\pi^5\left(\frac{8}{63}-\sum_{u=1}^{\infty}\Big[\text{cosech}^2(\pi Bu)\left(2\coth^4(\pi Bu)\right.\right.$$
$$\left.\left.+11\coth^2(\pi Bu)\text{cosech}^2(\pi Bu)+2\text{cosech}^4(\pi Bu)\right)\Big]\right),$$

and it turns out that for $B=1$, the summation in u equals the constant term in this lattice sum, and as a result $L[6,0]$ cancels to zero.

Additionally, in the case of square lattices,

$$L[4,0]\simeq -3.00919,\quad L[8,0]\simeq -3413.73,\quad L[12,0]\simeq -1.25117\times 10^7,$$

C. Justifying The Form Of Expansion For Centrally Symmetric Shapes

In the context of the shape function, central symmetry of the shape indicates that $f(\theta+\pi)=f(\theta)$.

First, consider the summation terms in (3.24) and (3.25). When $\delta=\xi=0$ or $\delta+\xi$ is even, displacement gradient moments of odd order could possibly appear in this term only when $\alpha+\beta$ is even. This can be observed by examining the coefficient $\hat{C}_{\delta\xi\alpha\beta}$ as defined in (3.7), dividing the range of integration into two parts - one for $\hat{\theta}\in[0,\pi)$ and the other for $\hat{\theta}\in[\pi,2\pi)$, and using the substitution $\hat{\theta}=\psi+\pi$ in the integral from π to 2π. By making use of trigonometric angle sum identities and the fact that $f(\psi+\pi)=f(\psi)$ due to central symmetry, $\hat{C}_{\delta\xi\alpha\beta}$ can be transformed into an integral multiplied by the factor $1+(-1)^{\delta+\xi+\alpha+\beta}$.

Thus, with $\delta+\xi$ being even, $(-1)^{\delta+\xi+\alpha+\beta}=-1$ when $\alpha+\beta$ is odd and so $\hat{C}_{\delta\xi\alpha\beta}=0$. Therefore, for spherically symmetric fibre cross sections with $\delta+\xi$ being even, only terms within the quadruple sum where $\alpha+\beta$ is even will be non-trivial.

With this established, notice next that each moment in the quadruple sum term is multiplied by a lattice sum. It transpires that for every combination of α, β, i and j where $i+j$ is odd and $\alpha+\beta$ is even, at least one of the inputs of the lattice sum multiplying $W_{ij}^{(k)}$ is odd. All such scenarios are outlined in Table 2. As established earlier, the lattice sum evaluates to zero if either

α	β	i	j	Reason lattice sums are trivial
Even	Even	Odd	Even	$i+\alpha$, $i+\alpha+2$ and $j+\beta+1$ are all odd
Odd	Odd	Even	Odd	$i+\alpha$, $i+\alpha+2$ and $j+\beta+1$ are all odd
Even	Even	Even	Odd	$i+\alpha+1$, $j+\beta$ and $j+\beta+2$ are all odd
Odd	Odd	Odd	Even	$i+\alpha+1$, $j+\beta$ and $j+\beta+2$ are all odd

Table 2: List of possible scenarios where both $\alpha+\beta$ is even and $i+j$ is odd and how each scenario causes the lattice sum terms in (3.24) and (3.25) to be trivial

of its inputs is odd. Therefore, no moments of odd order will appear in the quadruples sum terms in even ordered ($\delta+\xi$ even) equations.

This leaves the displacement gradient moment expansion of the shape factor (3.12) and (3.13) as the only terms that can potentially involve moments of odd order. Note from the form of expansion that the shape factor term will not include any such moments if the $D_{ij}^{\delta\xi}$ coefficients are zero when $i+j$ is odd (hereon in described as coefficients of odd order). It transpires from the process discussed in Appendix A that the coefficients of odd order and those of even order separate into two subsystems. Therefore, if all coefficients of odd order are to be zero,

the subsystem of such coefficients should be homogeneous - i.e. no terms independent of the coefficients with indices totalling an odd number should be present in the subsystem.

Firstly note that since $\delta+\xi$ is even, the only inhomogeneous Laplace type condition one obtains from (A) is guaranteed not to involve any odd ordered coefficients. Therefore, it just remains to be shown that the equations in the system from Appendix A related to odd ordered coefficients are homogeneous. This requires the $A_m^{\delta\xi}$ and $B_m^{\delta\xi}$ terms to be zero when m is odd. When m is odd these reduce down to

$$\hat{A}_m^{\delta\xi} = \int_0^{2\pi} \cos^\delta\hat{\theta}\sin^\xi\hat{\theta}\cos m\hat{\theta} f^{(\delta+\xi+2-m)}(\hat{\theta})d\hat{\theta},$$
$$\hat{B}_m^{\delta\xi} = \int_0^{2\pi} \cos^\delta\hat{\theta}\sin^\xi\hat{\theta}\sin m\hat{\theta} f^{(\delta+\xi+2-m)}(\hat{\theta})d\hat{\theta},$$

where

$$\hat{A}_m^{\delta\xi} = -2m\pi\delta!\xi!(\delta+\xi+2-m)A_m^{\delta\xi}, \quad \hat{B}_m^{\delta\xi} = -2m\pi\delta!\xi!(\delta+\xi+2-m)B_m^{\delta\xi}.$$

As was the case when examining $\hat{C}_{\delta\xi\alpha\beta}$, splitting the range of integration into two parts - one for $\hat{\theta}\in[0,\pi)$ and the other for $\hat{\theta}\in[\pi,2\pi)$ then substituting $\hat{\theta}=\psi+\pi$ into the latter and making further use of the central symmetry of f and using trigonometric angle sum identities, the above can be rewritten as single integrals featuring coefficient $1+(-1)^{m+\delta+\xi}$. Since m is odd and $\delta+\xi$ is even, $(-1)^{m+\delta+\xi}=-1$ and thus the coefficient of the integral is zero, meaning $A_m^{\delta\xi}$ and $B_m^{\delta\xi}$ are also zero. Therefore, any sub system of equations in coefficients $D_{ij}^{\delta\xi}$ where $i+j$ is odd will be homogeneous in these coefficients and hence the solution for this subset of coefficients will be trivial. This means that, when $\delta+\xi$ is even, the expansion of $J_{\delta\xi}(\boldsymbol{y})$ will not feature any powers of the coordinate basis of odd order.

With regards to the shape factor, this results in no displacement gradient moments of odd order appearing in (3.12) and (3.13) when $\delta+\xi$ is even and the fibre cross section shape is centrally symmetric. Therefore, in this case, no fractional powers of the volume fraction ϕ shall appear in the system, which means that asymptotically expanding the moments and $\Gamma(\gamma_1)$ in powers of $\phi^{1/2}$ is unnecessary. Instead, one can expand in powers of ϕ.

References

1. Milton, G.W. 2001. *The theory of composites*. Cambridge University Press, Cambridge. 1st Ed.
2. Bakhvalov, N. and Panasenko G. 1989. *Homogenisation: Averaging Processes in Periodic Media: Mathematical Problems in the Mechanics of Composite Materials*. Springer.
3. Edelstein, A.S. and Cammarata, R.C. (Eds) 1996. *Nanomaterials: Synthesis, properties and applications*. CRC Press, New York. 2nd Ed.
4. Sabina, F. J., Bravo-Castillero, J., Guinovart-Díaz, R., Rodríguez-Ramos, R. and Valdiviezo-Mijangos, O. C. 2002. Overall behaviour of two-dimensional periodic composites. *Int. J. Solids Structures* 39, 483Ű497.
5. Parnell, W.J and Abrahams, I.D. 2006. Dynamic homogenization in periodic fibre reinforced media. Quasi-static limit for SH waves. *Wave Motion* 43, 474-498.
6. Parnell, W.J and Abrahams, I.D. 2008. Homogenization for wave propagation in periodic fibre-reinforced media with complex microstructure. I-Theory. *J. Mech. Phys. Soilds* 56, 2521-2540.
7. Iwakuma, T. and Nemat-Nasser, S. 1983. Composites with periodic microstructure. *Comp. Structures* 16, 13-19.
8. Nemat-Nasser, S. and Hori, M. 1999. Micromechanics: Overall properties of Heterogeneous materials. North-Holland, Amsterdam.
9. Helsing, J. 1995. An integral equation method for elastostatic of periodic composites. *J. Mech. Phys. Solids* 43, 815-828.
10. Moulinec, H., Suquet, P. 1994. A fast numerical method for computing the linear and nonlinear properties of composites. *C. R. Acad. Sci. II* 318, 1417-1423.
11. Michel, J., Moulinec, H and Suquet, P. 1999. Effective properties of composite materials with periodic microstructure: a computational approach. *Comput. Meth. Appl. Mech. Eng* 172, 109-143.

12. Bonnet, G. 2007. Effective properties of elastic periodic composite media with fibers. *J. Mech. Phys. Solids* 55, 881-899.
13. Kushwaha, M.S., Halevi, P., Martínez, G., Dobrzynski, L. and Djafari-Rouhani, B. Acoustic band structure of periodic elastic composites. *Phys. Rev. Lett.* 71, 2022.
14. Zalipaev, V.V and Movchan, A.B and Poulton, C.G and McPhedran, R.C. 2002. Elastic waves and homogenization in oblique periodic structures. *Proc. R. Soc. A* 458, 1887-1912.
15. Craster, R. V., Kaplunov, J. and Pichugin, A.V. 2010. High-frequency homogenization for periodic media. *Proc. Roy. Soc. A* 466, 2341-2362.
16. Hussein, M.I., Leamy, M.J. and Ruzzene, M. 2014. Dynamics of phononic materials and structures: Historial origins, recent progress and future outlook. *Appl. Mech. Rev.* 66, 040802.
17. Parnell, W.J and Abrahams, I.D. 2008. A new integral equation approach to elastodynamic homogenization. *Proc. R. Soc. A.* 464. 1461-1482.
18. Brazier-Smith, P.R. 2002. A unified model for the properties of composite materials. In *Proc. IUTAM Symposium on scattering and diffraction in fluid mechanics and elasticity*, Manchester, UK, 16Ű20 July 2000. Dordrecht, The Netherlands: Kluwer.
19. McIver, R. and Krynkin, A.. 2009. Approximations to wave propagation through a lattice of Dirichlet scatterers. *Waves in Random and Complex Media* 19, 347-365.
20. McIver, R. and Guo, S. 2011. Propagation of elastic waves through a lattice of cylindrical cavities. *Proc. R. Soc. A.* 467, 2962-2982.
21. Mura, T. 1982. *Micromechanics of Defects in Solids*. Kluwer.
22. Parnell, W.J., Abrahams, I.D and Brazier-Smith, P.R 2010. Effective Properties of a Composite Half-Space: Exploring the Relationship Between Homogenization and Multiple-Scattering Theories. Q. J. Mech. Applied Math. 63, 145-175.
23. Gielis, J. 2003, A generic geometric transformation that unifies a wide range of natural and abstract shapes. Am. J. Botany 90, 333-338.
24. Gradshteyn, I. S. and Ryzhik, I. M., editor Zwillinger, D. 2014, Table of Integrals, Series, and Products, Eigth Edition. Associated Press.